Articles

Truncation of the Amino Terminus of Human Apolipoprotein A-I Substantially Alters Only the Lipid-Free Conformation†

Danise P. Rogers,‡ Christie G. Brouillette,*,‡,§,▽ Jeffrey A. Engler,*,‡ Susan W. Tendian,§ Linda Roberts,|| Vinod K. Mishra,⊥ G. M. Anantharamaiah,‡,⊥ Sissel Lund-Katz,# Michael C. Phillips,# and Marjorie J. Ray‡

Biochemistry Department, Southern Research Institute, Birmingham, Alabama 35209, Department of Biochemistry and Molecular Genetics and Department of Medicine and Atherosclerosis Research Unit, University of Alabama at Birmingham Medical Center, Birmingham, Alabama 35294, Department of Chemistry, California State University at Sacramento, Sacramento, California 95819, and Department of Biochemistry, The Medical College of Pennsylvania and Hahnemann University, Philadelphia, Pennsylvania 19129

Received July 29, 1996; Revised Manuscript Received October 29, 1996⊗

ABSTRACT: An amino-terminal deletion mutant (residues 1−43) of human apolipoprotein A-I (apo hA-I) has been produced from a bacterial expression system to explore the structural and functional role of these amino acids, encoded by exon 3, in apo hA-I. Lipid binding of apo Δ(1−43)A-I and lipid binding of apo hA-I are very similar as assessed by surface activity, lipid association with palmitoyloleoylphosphatidylcholine (POPC) vesicles, and lipid association with plasma lipoproteins. Preliminary kinetic measurements appear to show that the reactivity of lecithin:cholesterol acyltransferase (LCAT) with the mutant is slightly decreased compared to wild-type apo hA-I. Collectively, these results indicate that the N-terminal region is not necessary for lipid binding or activation of LCAT. In contrast, there are significant structural differences between lipid-free apo Δ(1−43)A-I and apo hA-I, as judged by denaturant-induced unfolding, binding of the fluorescent probe 1-anilinonaphthalene-8-sulfonate, surface balance measurements, and far- and near-ultraviolet circular dichroic spectroscopy. All spectral and physical measurements indicate apo Δ(1−43)A-I has a folded, tertiary structure, although it is significantly less stable than that of apo hA-I. It is concluded that the N-terminal 43 residues are an important structural element of the lipid-free conformational state of apo hA-I, the absence of which induces a fundamentally different fold for the remaining carboxy-terminal residues, compared to those in native apo hA-I.

Human apolipoprotein A-I (apo hA-I)[1] is the major protein of high-density lipoprotein (HDL), comprising about 70% of the total HDL protein. HDL levels, quantified by either cholesterol or apolipoprotein A-I content, are a better predictor of coronary artery disease (CAD), as a single parameter in assessing risk, than any other single risk factor (Breslow, 1989; Gordon et al., 1977). Studies of human apo A-I in transgenic animals susceptible to atherosclerosis have established that apo A-I is responsible for the protective effect of HDL against the onset of CAD (Schultz et al., 1993; Warden et al., 1993; Plumb et al., 1994). During the course of HDL catabolism, particles are continually remodeled by the transfer and exchange of lipid components between lipoproteins and by the action of enzymes, most notably the plasma enzyme lecithin:cholesterol acyltransferase (LCAT). Apo A-I is the most potent activator of LCAT, which catalyzes the conversion of free cholesterol to cholesterol ester (Fielding et al., 1972), thereby facilitating the clearance of cholesterol from peripheral tissues through the liver in a process termed reverse cholesterol transport (Glomset, 1968; Forte & McCall, 1994). In addition, apo A-I is thought to be an important ligand in the binding of HDL to cellular membranes (Oram, 1986; Sviridov et al., 1996), and,

† This work was supported by Grants HL34343 and HL22633 from the National Institutes of Health. Synthesis of oligonucleotides for site-directed mutagenesis and DNA sequencing was supported in part by NCI Grant P50 CA13148 to the UAB Comprehensive Cancer Center. Use of computer programs used for analysis of DNA sequences (from the Genetics Computer Group, Madison, WI) was supported in part by NIAID Grant P50 AI27767.

* To whom correspondence should be addressed.

‡ Department of Biochemistry and Molecular Genetics, University of Alabama at Birmingham Medical Center.

§ Biochemistry Department, Southern Research Institute.

▽ Present address: Center for Macromolecular Crystallography, University of Alabama at Birmingham, Room 290 BHSB, 1918 University Blvd., Birmingham, Alabama, 35294-0005.

|| Department of Chemistry, California State University at Sacramento.

⊥ Department of Medicine and Atherosclerosis Research Unit, University of Alabama at Birmingham Medical Center.

Department of Biochemistry, The Medical College of Pennsylvania and Hahnemann University.

⊗ Abstract published in *Advance ACS Abstracts,* December 1, 1996.

[1] Abbreviations: ANS, 1-anilinonaphthalene-8-sulfonate; apo A-I, apolipoprotein A-I; apo hA-I, human apo A-I; apo Δ(1−43)A-I, mutant of apo hA-I missing residues 1−43; CAD, coronary artery disease; CD, circular dichroism; DMPC, dimyristoylphosphatidylcholine; HDL, high-density lipoprotein; IPTG, isopropyl β-thiogalactopyranoside; LCAT, lecithin:cholesterol acyltransferase; LDL, low-density lipoprotein; PBS, phosphate-buffered saline containing 0.02 M sodium phosphate, 0.15 M sodium chloride, 0.02% sodium azide, and 1 mM ethylenediaminetetraacetic acid; PMSF, phenylmethanesulfonyl fluoride; POPC, palmitoyloleoylphosphatidylcholine; rLp, reconstituted lipoprotein(s); TLC, thin-layer chromatography; VLDL, very low density lipoprotein.

S0006-2960(96)01876-4 CCC: $14.00

recently, an apo A-I-specific receptor has been identified in liver and nonplacental steroidogenic tissues (Acton et al., 1996).

Structural studies of apo A-I employing conformationally sensitive monoclonal antibodies (Calabresi et al., 1993; Collet et al., 1991), fluorescence spectroscopy (Jonas et al., 1990), and ^{13}C NMR of labeled lysines (Sparks et al., 1992a,b) are consistent with an adaptable or flexible amino terminus. The antibody and NMR studies also demonstrated that conformational changes in the amino terminus occur during the conversion of apo A-I from the lipid-free to the lipid-bound form (Marcel et al., 1991; Meng et al., 1993; Sparks et al., 1992a,b). In these studies, the definition of the "amino terminal region" is necessarily different. Conformational studies using intrinsic fluorescence typically define the amino terminus through residue 108, because it has not been possible to assign a unique signal to each of the 4 tryptophans located between residues 7 and 109. Similarly, proteolysis studies have demonstrated that residues 1 through 115 are protected from proteolysis in the lipid-free form, thus reporting on essentially the same block of residues (reviewed in Brouillette & Anantharamaiah, 1995). In contrast, the amino terminus can be subdivided into an extreme amino-terminal region defined by residues 1 through 15 (Curtiss & Smith, 1988; Marcel et al., 1991) and a larger domain approximately encompassing residues 14−90 (Bergeron et al., 1995), based on published studies using monoclonal antibodies which recognize epitopes in these two regions.

Mutagenesis or "protein dissection" by proteolysis, the replacement or deletion of specific residues, has been shown to be a powerful tool in studying the structure and function of a variety of proteins, including apo A-I (Bruhn & Stoffel, 1991; Ji & Jonas, 1995; Sorci-Thomas et al., 1994; Minnich et al., 1992; Schmidt et al., 1995). This approach can define more precisely the local structure of particular regions in proteins but, until now, has not been used to directly examine the N-terminal region of apo A-I. In the studies described here, the N-terminal residues 1 through 43 have been selected as a single block for deletion; the removal of these residues provides the most direct way to elucidate the structural and functional importance of this region.

The rationale for deleting the first 43 residues comes from the genomic as well as the amino acid structure of apo A-I. Exon 3 encodes residues 1−43 in apo A-I. This region is more highly conserved across different species than is the remainder of the protein, which is encoded by exon 4, suggesting it may have a function other than, or in addition to, lipid binding. The residues in exon 3 have been described as having a different internal sequence homology (McLachlan, 1977; Li et al., 1988) as well as containing a completely different amphipathic helical class than those derived from exon 4 (Segrest et al., 1992). In addition, sequence analyses distinguish the amino terminus from the remainder of the protein in that some nonhelical secondary structure is predicted (Marcel et al., 1991; Nolte & Atkinson, 1992; Segrest et al., 1992, 1994). Taken together these studies identify the amino terminus as a unique region of apo hA-I which has not been well characterized or understood.

The emphasis of the present study is to describe the differences in the lipid-free conformations of apo Δ(1−43)A-I relative to native apo hA-I through the use of multiple techniques, including denaturant-induced unfolding measured by spectroscopic methods, ANS binding, near- and far-UV CD, and surface balance measurements. The similarities in the lipid-bound conformations are also examined through a series of experiments that test function including monolayer and lipid vesicle binding, and LCAT activation, while future studies will focus on the subtle differences in the lipid-bound conformations. The present studies indicate that residues 1−43 are necessary to maintain and stabilize the structure of lipid-free apo hA-I and also suggest they play a key role in the conformational switch between the lipid-free and lipid-bound forms.

EXPERIMENTAL PROCEDURES

Preparation of Human Apo A-I. Human apo A-I (apo hA-I) in the methionine-reduced state (Anantharamaiah et al., 1988) was purified by the method of Hughes et al. (1988), which consists of density gradient ultracentrifugation to obtain the HDL density fraction, delipidation of the HDL, and preparative reversed phase high-performance liquid chromatography; the purified protein was then lyophilized for storage at −20 °C. Lyophilized protein was solubilized, as needed, in 6 M guanidine hydrochloride in PBS (0.02 M phosphate, 0.15 M NaCl, 0.02% NaN_3, and 1 mM EDTA, pH 7.4) and then dialyzed against PBS containing 10 μM D,L-α-tocopherol, 50 μM ascorbic acid, and 1 mM EDTA. An extinction coefficient of 1.13 mL/(mg·cm) at 280 nm was used for determining apo hA-I concentration in 6 M guanidine hydrochloride (Pownall & Massey, 1986).

Construction and Expression of Apo Δ(1−43)A-I Containing Vector. The apo hA-I cDNA that encodes the prepropeptide form of apo A-I (Cheung & Chan, 1983) was cloned into the plasmid pGEMEX (Promega, Madison, WI). The prepro coding region of the apo A-I cDNA was removed by PCR amplification; *Xba*I and *Hin*dIII cleavage sites were included at the upstream and downstream ends (respectively) of the mature apo hA-I open reading frame. Single-stranded DNA from this plasmid was prepared by standard methods (Vieira & Messing, 1987) using helper phage VCSM13 (Stratagene, San Diego, CA) and used for site-directed mutagenesis (Zoller & Smith, 1983), using the oligonucleotide 5′-TAAGAAGGAGATATACATATGCTAAAGCTCCTTGACAAC-3′ (sense strand) to delete nucleotide sequences encoding amino acids 1 through 43. Mutants were identified by colony hybridization using the mutagenic oligonucleotide, and their identity was confirmed by double-strand dideoxynucleotide DNA sequencing [United States Biochemical (USB), Cleveland, OH] of the resulting plasmid DNA. The mutant gene product was expressed in *E. coli* BL21/DE3 cells (Studier & Moffat, 1986) by growth of the transformed bacteria in sterile DYT medium (10 g of casein peptone, 10 g of yeast extract, 5 g of NaCl, and 2 pellets of NaOH per liter) with 100 μg/mL ampicillin to an OD_{600} = 0.9−1.0. The chromosomal copy of the bacteriophage T7 RNA polymerase gene was then induced with 1 mM IPTG. After 4 h, the induced *E. coli* cells were collected by centrifugation and resuspended in sterile phosphate-buffered saline (PBS) containing a mixture of antioxidants (1 μM α-tocopherol, 50 μM ascorbic acid) and protease inhibitors (5 mM PMSF, 1 mM EDTA, 0.2% NaN_3).

Purification and Characterization of Apo Δ(1−43)A-I. The resuspended *E. coli* cell pellet was lysed by French press. Dimyristoylphosphatidylcholine (DMPC; Avanti Polar Lipids, Inc., Alabaster, AL) was added to the supernatant

containing recombinant protein to a final concentration of 40 mg/mL and mixed on an orbital shaker overnight at room temperature. A two-step gradient was used to float the DMPC/protein complexes by overlaying the supernatant/DMPC mixture (adjusted to a density of 1.3 g/mL with KBr) with a KBr buffer (density 1.2 g/mL). Centrifugation in 39.5 mL tubes was accomplished with a 70 Ti rotor (Beckman Instruments) at 70 000 rpm for 22 h at 24 °C. Greater than 90% of the recombinant apo A-I was found to be in the top layer, comigrating with the lipid. The resulting top layer was delipidated by extraction with organic solvent (Radin, 1981), followed by dialysis at 4 °C against ammonium bicarbonate (4.5 g/L). Analytical HPLC (Hughes et al., 1988) and SDS−PAGE were performed on the dialyzed recombinant apo A-I. If the recombinant protein was less than 95% pure by either of these criteria, it was subjected to preparative HPLC as described above for the preparation of apo hA-I. The recombinant apo A-I was stored lyophilized and solubilized when needed as indicated for apo hA-I.

SDS−PAGE on 12% or 15% gels was run in a Bio-Rad mini-gel apparatus and protein stained by Coomassie Brilliant Blue R-250 (Sigma, St. Louis, MO) or by a standard silver staining procedure. Western blotting of SDS−PAGE gels was accomplished after electroblotting to nitrocellulose and exposure to a polyclonal antibody raised against apo hA-I (Southern Biotechnology Association, Birmingham, AL). Isoelectric focusing (IEF) was carried out in the pH range 3−10 with a Pharmacia Phast System in the presence of 3 M urea, 1% Triton X-100, and 2% β-mercaptoethanol. The gels were stained with Coomassie Brilliant Blue R-250 stain and destained by the manufacturer's instructions. Quantitative amino acid analysis and N-terminal sequencing were performed by the Glycoprotein Analysis Core Facility at the University of Alabama at Birmingham Medical Center. An extinction coefficient at 280 nm in 6 M guanidine hydrochloride for apo Δ(1−43)A-I was determined by quantitative amino acid analysis to be 0.991 mL/(mg·cm), which corresponds to the calculated extinction determined from the amino acid composition.

Preparation and Characterization of rLp Complexes Containing Apo hA-I or Apo Δ(1−43)A-I. Palmitoyloleoylphosphatidylcholine (POPC)-containing rLp were formed by drying an ethanolic solution of POPC in a small test tube with a stream of argon followed by further drying under vacuum for at least 2 h. Sodium cholate in PBS buffer was added to the dried powder at a 4:1 sodium cholate to POPC molar ratio followed by incubation at room temperature for a minimum of 2 h. Apo hA-I or apo Δ(1−43)A-I in PBS buffer was added to give a 100:1 POPC to protein molar ratio, and the mixture was incubated for a minimum of 5 h at room temperature and then dialyzed overnight against PBS buffer at 4 °C with at least 3 changes of 4 L each. The dialysis tubing used has a molecular mass cutoff of 50 000 daltons which allowed soluble, uncomplexed protein to be removed. The rLp isolated from this preparation were not contaminated with free, uncomplexed apo A-I, as confirmed by its absence on native electrophoresed gradient gels (data not shown). The protein content of the isolated rLp was determined using a modified version of the Lowry protein assay where 10% SDS was added to the reaction mixture to reach a final concentration of 0.1% or by UV absorbance at 280 nm in 6 M guanidine hydrochloride. The phospholipid content of the isolated rLp was determined using an enzymatic assay (Warnick, 1986). Native gradient gel electrophoresis (GGE) of the isolated rLp was accomplished on a 3−20% linear acrylamide gradient gel (Brouillette et al., 1984). The average protein:POPC molar composition of rLp isolated from five different preparations of each apolipoprotein was 1:100(±4) for apo hA-I and 1:109(±7) for apo Δ(1−43)A-I.

Lecithin:Cholesterol Acyltransferase (LCAT) Purification. The procedure of Albers et al. (1986) was used with minor modifications. Fresh, normolipidemic human plasma was ultracentrifuged at 1.21 g/mL density. Following dialysis, the LCAT-containing fraction was subjected to Affi-Gel Blue chromatography and DE-52 chromatography. LCAT was eluted from the DE-52 column with a 75−200 mM NaCl gradient. SDS−PAGE showed ≥90% purity with no apo hA-I contamination.

LCAT Activity Assay. The assay used for determining the ability of the apolipoprotein to activate LCAT utilized preformed, isolated rLp as the substrate, similar to that reported by others (Albers et al., 1986; Matz & Jonas, 1982). The substrate rLp were prepared at an initial POPC:cholesterol:apolipoprotein molar ratio of 100:4:1 with either apo hA-I or apo Δ(1−43)A-I as described above for POPC-only rLp except that an ethanolic solution of cholesterol, which included 1.8 μg of [^{3}H]cholesterol, or 20% of the total cholesterol (specific activity = 0.1 mCi/μg), was dried down with the POPC. Isolated cholesterol-containing rLp contained no free apolipoprotein and were identical in size distribution, as assessed by native GGE, to the POPC-only rLp. The methods of compositional analysis for protein and POPC were identical to those for the POPC-only rLp. Cholesterol (Ch) content of isolated complexes was determined by their specific radioactivity using appropriate standards. The average protein:POPC:Ch molar composition of rLp isolated from up to nine different preparations of each apolipoprotein was 1:98(±5):2(±0.2) for apo hA-I and 1:95(±8):2(±0.4) for apo Δ(1−43)A-I.

The substrate rLp were equilibrated at 37 °C for 5 min in a pH 8.0, 10 mM Tris buffer containing 300 μg/mL bovine serum albumin, 5 mM β-mercaptoethanol, 150 mM NaCl, and 0.01% EDTA. The reaction was initiated by the addition of LCAT and followed with incubation for 5, 10, 20, 30, and 50 min at 37 °C. The final volume of the enzyme reaction mixture ranged from 100 to 200 μL and contained 0.25−10 μg/mL protein. Reactions were run in triplicate and terminated by applying 20 μL of the reaction mixture to silica gel thin-layer chromatography (TLC) plates. The TLC plates were developed using a solvent system composed of hexane/chloroform, 2:1 (v/v). Cholesterol and cholesteryl oleate standards were visualized by immersing the TLC plate in a 3% cupric acetate, 8% phosphoric acid buffer, and then applying heat. The positions of the standards were used to determine where to cut the corresponding tritiated reaction spots, which were subsequently added to scintillation fluid and counted on a Packard Tri Carb 4530. Only the linear portion of the reaction curve was used to determine initial velocities, V_o, and ≤5% conversion to cholesterol ester was observed during the time course used.

A nonlinear least-squares algorithm was used to fit the data to the Michaelis−Menten equation (eq 1):

$$V_o = \frac{V_{max}[\text{apoprotein}]}{K_m + [\text{apoprotein}]} \quad (1)$$

from which apparent V_{max} and K_m values were determined. A Student's *t*-test was applied to the calculated kinetic parameters to determine their statistical significance. Reported apparent V_{max} values are normalized to units of enzyme activity where 1 unit = 1 nmol of cholesterol ester formed/mg of LCAT/h as previously described (Sparks et al., 1995).

Circular Dichroism Spectroscopy of Apo hA-I and Apo Δ(1−43)A-I. The CD spectra were recorded with an AVIV 62DS spectropolarimeter interfaced to a personal computer (80386) and standardized using a solution of 0.1% (w/v) *d*-10-camphorsulfonic acid. Spectra were recorded on solutions containing 0.5−25 μM protein in PBS (without NaN_3 or EDTA), thermostated at 25 °C. To more easily compare their lipid-free spectra, the concentrations of protein were kept low, and the aggregation state was checked by chemical cross-linking (data not shown). Since the aggregation states of the proteins are similar, the possible contribution from differences in aggregation state to the CD signal is insignificant (Osborne & Brewer, 1977). The spectra were concentration-independent in this concentration range for both proteins. The dynode voltage of each sample was also recorded at the same time as the CD spectrum and was used as an internal standardization of the protein concentration which was determined spectroscopically as described above. The CD spectra were measured every 0.5 nm with 0.5 s averaging per point, and a 2 nm bandwidth. A 0.01 cm path-length cell was used for far-UV spectra; a 10 mm path-length cell was used for near-UV spectra. Spectra were signal-averaged by adding at least eight scans and base-line-corrected by subtracting a spectrum for the buffer obtained in an identical manner. The spectra were normalized to molar residue ellipticity using a mean residue weight of 115.2 Da for apo hA-I and 115.7 Da for apo Δ(1−43)A-I.

Distribution of Exogenous Apo hA-I and Apo Δ(1−43)A-I among Human Plasma Lipoproteins. Approximately 2 μg of protein was radioiodinated by the iodine monochloride method using 0.5 mCi of ^{125}ICl (McFarland, 1958). Unreacted ^{125}ICl was removed by chromatography on a Bio-Rad Econo-Pac 10 DG column. The radiolabeled protein was added to 0.5 mL of plasma at a 1:500 (w/w, based on protein, which was 27 mg/mL in plasma) ratio. The mixture was incubated for 18 h at 4 °C or for 1 h at 37 °C. The volume of the mixture was made up to 1.5 mL by adding 150 mM sodium chloride (pH 7.4). The density of the mixture was adjusted to 1.21 g/mL with solid KBr and transferred to a 5 mL polyallomer quick-seal Beckman ultracentrifuge tube. The mixture was overlaid with sodium chloride solution (150 mM, pH 7.4). The tube was centrifuged at 80 000 rpm for 44 min at 20 °C in a Beckman Ultracentrifuge (L8-80M) using a VTi80 rotor. After centrifugation, fractions (0.2 mL) were collected by downward fractionation, and radioactivity (gamma counter, COBRA; Auto-Gamma, Packard Instrument Co., IL), protein (absorbance at 280 nm), and cholesterol (absorbance at 505 nm; cholesterol/HP reagent; Boehringer Mannheim Corp., IN) were quantitated.

Binding of Apo hA-I and Apo Δ(1−43)A-I to POPC Vesicles. The procedure of Spuhler et al. (1994) was followed in which aliquots of apolipoprotein ranging in concentration from approximately 1 to 7 μM were vortexed and subjected to six freeze−thaw cycles (−70 °C) with buffer-hydrated 9.2 mM POPC over 1 h, followed by further vortexing. The resulting multilamellar vesicles were centrifuged at 4 °C for 2 h at 120000*g*. The equilibrium concentration of unbound apolipoprotein was determined from the UV spectrum of the clear supernatant. Apo hA-I and apo Δ(1−43)A-I do not disrupt POPC vesicles into smaller, less dense particles since no lipid was detectable in the supernatant after centrifugation. The entrapment of unbound apolipoprotein within the POPC vesicular aqueous compartments does not affect the determination of the binding constant since the experimental protocol allows for equilibration of the unbound protein concentration; the trapped apolipoprotein concentration is, therefore, the same as the concentration found in the supernatant following centrifugation. It has previously been shown (Spuhler et al., 1994) that any possible residual lipid remaining in the supernatant following centrifugation can be easily corrected for by performing the same experiment in the absence of apolipoprotein to determine the optical density of the resulting protein-free supernatant. The experimental data are best fit to a simple partition equilibrium according to eq 2:

$$X_b = K_a c_{eq} \quad (2)$$

where X_b, K_a, and c_{eq} denote the molar ratio of bound apolipoprotein to total POPC, the equilibrium binding constant, and the equilibrium concentration of unbound apolipoprotein, respectively. The slope of the linear plot of X_b vs c_{eq} is equal to K_a. The binding free energy can be calculated by eq 3, in which the cratic contribution of water to ΔG is accounted for by the factor of 55.5 (Spuhler et al., 1994):

$$\Delta G = -RT \ln (55.5 K_a) \quad (3)$$

Reversible Equilibrium Unfolding/Refolding by Difference Spectroscopy. Urea-induced unfolding of lipid-free apo hA-I and apo Δ(1−43)A-I was monitored by circular dichroism [AVIV 62DS spectropolarimeter (AVIV, Lakeside NJ)], fluorescence [Aminco-Bowman Series 2 fluorometer (SLM-Aminco, Rochester, NY)], and ultraviolet absorbance [Cary 3E UV/visible spectrophotometer (Varian Australia Pty. Ltd., Victoria, Autstralia)] spectroscopies. Urea stock solutions (10 M) made from Ultrapure urea (Gibco BRL, Grand Island, NY) in PBS, pH 7.4, were prepared fresh for each experiment, and the concentration was verified by refractive index measurements (Warren & Gordon, 1966) using an Abbe Refractometer (American Optical Corp., Buffalo, NY). The concentrations of apo hA-I and apo Δ(1−43)A-I were kept constant at 0.1 mg/mL, which is below the aggregation concentration as assessed by Barbeau et al. (1979) for apo hA-I and as determined from our current studies for apo Δ(1−43)A-I (data not shown). Protein samples (0.1 mg/mL) were incubated with various concentrations of urea, ranging from 0 to 4.0 M, at 4 °C, for at least 15 h to allow samples to reach equilibrium.

Circular dichroic spectra were obtained as described above, with a wavelength range of 250−205 nm, and a temperature-controller set at 20 °C. A 0.2 cm path-length cell was used for the far-UV spectra, and spectra were signal-averaged by adding at least five scans. The spectra were corrected by

subtracting the appropriate buffer or urea blanks obtained in a similar manner. Difference spectra were then generated by subtracting spectra of protein samples containing urea from the spectrum of protein samples in buffer alone (PBS, pH 7.4). The base-line-corrected spectra were normalized to molar ellipticity (ellip).

Fluorescence emission spectra and absorbance spectra were obtained as described elsewhere (Tendian et al., 1995). Difference spectra were obtained by subtracting spectra of protein samples containing urea from the spectrum of protein samples in buffer alone (Δfluor and Δabs, respectively).

Curve Fitting of Unfolding/Refolding Data. The data were fit to the two-state unfolding model (Santoro & Bolen, 1988) as described by the equation:

$$\text{F (folded)} \underset{K_D}{\rightleftharpoons} \text{U (unfolded)} \tag{4}$$

where K_D is the equilibrium constant that defines the unfolding equilibria. Curve fitting of the data was done as described in Tendian et al. (1995). The urea-dependent equilibrium constant of unfolding, for a two-state unfolding model, is represented by eq 5:

$$K_D = \exp[(\Delta G_{H_2O} - m_D[D])/-RT] \tag{5}$$

$$f_u = K_D/(1 + K_D) \tag{6}$$

$$f_u = (\Delta y - \Delta y_f)/(\Delta y_u - \Delta y_f) \tag{7}$$

Briefly, eqs 5 and 6 were used for global fits after converting ellip, Δfluor, or Δabs to f_u using eq 7, where Δy is the experimental spectroscopic measurement, Δy_f is the preunfolding value, Δy_u is the postunfolding value, [D] is the experimental denaturant concentration, ΔG_{H_2O} is the free energy difference between the native state and the unfolded state of the protein in water (in the absence of denaturant), m_D is a function of the steepness of the transition between the folded and unfolded states, and f_u represents the fraction of protein molecules in the unfolded state. $\Delta G_{H_2O}/m_D$ equals $[\text{urea}]_{1/2}$, which is the urea concentration at the midpoint of the unfolding transition (the concentration of native protein equals the concentration of unfolded protein). Δy_f and Δy_u were determined by linear regression of the first or last few data points in the unfolding curve according to eqs 8 and 9, respectively (Pace et al., 1989).

$$\Delta y_f = \Delta y_f^\circ + m_f[\text{urea}] \tag{8}$$

$$\Delta y_u = \Delta y_u^\circ + m_u[\text{urea}] \tag{9}$$

When not enough initial or final points were available to determine a folded or unfolded base line, m_f or m_u were set equal to zero and Δy_f° and Δy_u° were set equal to the average Δy of the available points. Eftink (1994) has shown through simulations of unfolding data that this assumption does not normally introduce unacceptable errors in the derived thermodynamic data. For the global fit analysis, multiple data sets including circular dichroic, emission, and absorption data for a given protein were used to determine a single set of thermodynamic parameters.

ANS (1-Anilinonaphthalene-8-sulfonate) Binding Measurements. ANS (1-anilinonaphthalene-8-sulfonate; Aldrich, Milwaukee, WI) binding experiments were carried out on solutions containing 50 μg/mL protein [1.8 μM for apo hA-I and 2.1 μM for apo Δ(1−43)A-I] and 250 μM ANS. Carbonic anhydrase (M_r 28 000) was used as a control (35 μg/mL, 1.4 μM) representing a typical water-soluble globular protein. In all cases, ANS was in at least 100-fold excess of the protein (mol/mol). ANS fluorescence was obtained at an excitation wavelength of 395 nm with a 5 nm slit width. Fluorescence spectra obtained were compared to ANS (250 μM) in PBS. Data were collected on a Shimadzu RF5000U spectrofluorophotometer connected to a DR-15 computer.

Surface Properties of Apo hA-I and Apo Δ(1−43)A-I. The relative affinities of the apo A-I molecules for the lipid−water interface were investigated using a surface balance technique employing prior procedures (Ibdah & Phillips, 1988; Phillips & Krebs, 1986). An insoluble monolayer of egg phosphatidylcholine (PC) was spread at the air−water interface (85 cm^2) in a circular Teflon dish containing 80 mL of phosphate-buffered saline (PBS: 5.65 mM Na_2HPO_4/3.05 mM NaH_2PO_4) at pH 7 and room temperature. The surface pressure (π) was monitored by the Wilhelmy plate technique using a 1 cm wide mica plate connected to a Cahn RTL recording electrobalance. Sufficient egg PC was spread from 9:1 (v/v) hexane/ethanol solution to give an initial surface pressure (π_i) in the range of 5−35 dyn/cm. Apo A-I dissolved in the above buffer containing 1.5 M guanidine hydrochloride was injected into the subphase to give an initial concentration of 5×10^{-5} g/dL; a small Teflon tube which projected through the monolayer into the aqueous subphase was used for this injection so that the egg PC monolayer was not disrupted. The presence of guanidine hydrochloride ensured that the protein molecules were initially present as random-coil monomers (Sparks et al., 1992a,b). The protein molecules renatured in the subphase as the guanidine hydrochloride were diluted to a final concentration of ≤1 mM. The solution was stirred continuously with a magnetic stirrer, and the increase in surface pressure ($\Delta\pi$) with time was recorded until a steady-state value of $\Delta\pi$ was reached. The $\Delta\pi$ values were plotted as a function of π_i. A linear extrapolation to $\Delta\pi = 0$ dyn/cm gave the exclusion pressure, or the value of π_i (±1 dyn/cm) at which the proteins were no longer able to penetrate into the egg PC monolayer.

The interfacial conformation of apo A-I was investigated by using a surface balance to determine the π−molecular area (A) isotherms for spread monolayers using procedures which have been described in detail elsewhere (Phillips & Krebs, 1986). The proteins were spread onto the surface of approximately 300 mL of PBS contained at pH 7 and room temperature in a Teflon trough (30 × 17.5 × 0.5 cm). After first dissolving the protein at 1 mg/mL in PBS containing 3 M guanidine hydrochloride, the apo A-I spreading solution was diluted with PBS to a final protein concentration (determined by A_{280}) of 60 μg/mL and a guanidine hydrochloride concentration of 180 mM. The guanidine hydrochloride was used to prevent self-association of the apo A-I molecules in the spreading solution, and its final concentration in the monolayer subphase was <1 mM; 0.5 mL of the protein solution was run down a glass rod to form the apo A-I monolayer at the air−water interface in the Teflon trough described above (Phillips & Krebs, 1986). After about 5 min, the surface area of the monolayer was reduced from the initial value of 1.8 m^2/mg using a movable barrier. The barrier was moved at 30 s intervals, and 20 readings of π and A were taken in a total elapsed time of 10 min. The

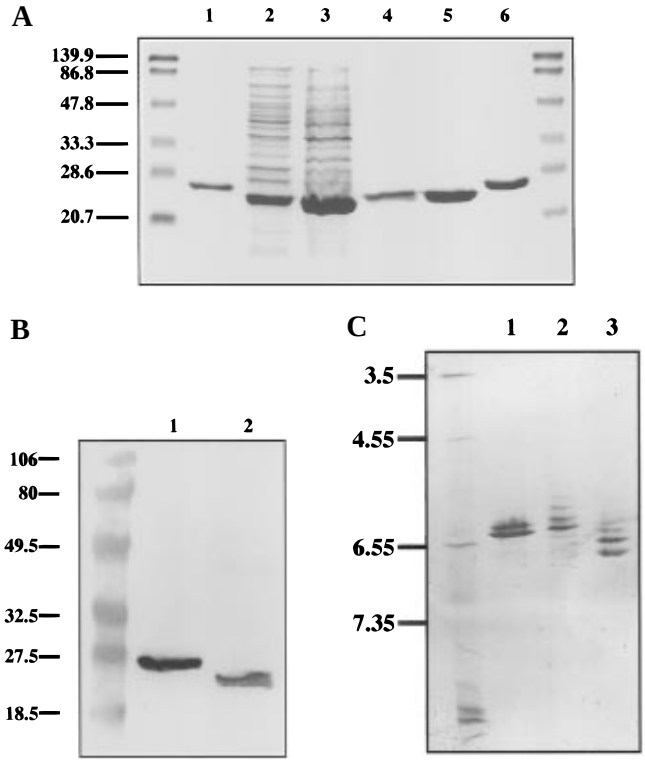

FIGURE 1: (A) SDS−PAGE of apo Δ(1−43)A-I before and after purification. Lanes 1 and 6, apo hA-I; lane 2, supernatant from *E. coli* cell lysate; lane 3, pellet from *E. coli* cell lysate; lanes 4 and 5, purified apo Δ(1−43)A-I; unlabeled lanes, molecular mass standards; molecular masses in kDa are indicated. (B) Western blot analysis of apo Δ(1−43)A-I and apo hA-I probed with a polyclonal antibody to apo hA-I. Lane 1, apo hA-I; lane 2, apo Δ(1−43)A-I; unlabeled lane, molecular mass standards; molecular masses in kDa are indicated. (C) Analytical IEF of apo Δ(1−43)A-I and apo hA-I. Lanes 1 and 2, apo hA-I; lane 3, apo Δ(1−43)A-I; unlabeled lane, Pharmacia p*I* 3−10 protein standards; p*I*s are indicated. The cathode is at the bottom.

surface pressure was measured with a Wilhelmy plate connected to a Cahn RTL recording electrobalance, as described above.

RESULTS

Expression, Purification, and Chemical Characterization of Apo Δ(1−43)A-I Expressed in E. coli. Up to 40 mg of apo Δ(1−43)A-I per liter of growth media was purified from the *E. coli* cell lysate by preparative reversed phase HPLC. The purity of the protein was assessed by several methods including SDS−PAGE, Western blotting, isoelectric focusing (IEF), analytical HPLC, amino acid analysis, and N-terminal sequencing. Analysis of the purified protein by SDS−PAGE (Figure 1A, lanes 4 and 5) and Western blot (Figure 1B, lane 2) shows the final product gave essentially a single band at an apparent molecular mass of 24 000 daltons, the size predicted for the apo Δ(1−43)A-I molecule. IEF analysis shows two major isoforms for apo Δ(1−43)A-I, which is also typical for apo hA-I (Figure 1C, lanes 1 and 3, respectively). As expected, the p*I* values of apo Δ(1−43)A-I isoforms are more basic than apo hA-I since fewer basic residues were eliminated than acidic residues (five basic and eight acidic residues). A single peak is observed by analytical reversed phase HPLC (Figure 2). This species is apparently the methionine-reduced form since deliberate oxidation of methionines with hydrogen peroxide to methionine sulfoxide shifts the HPLC retention time as expected

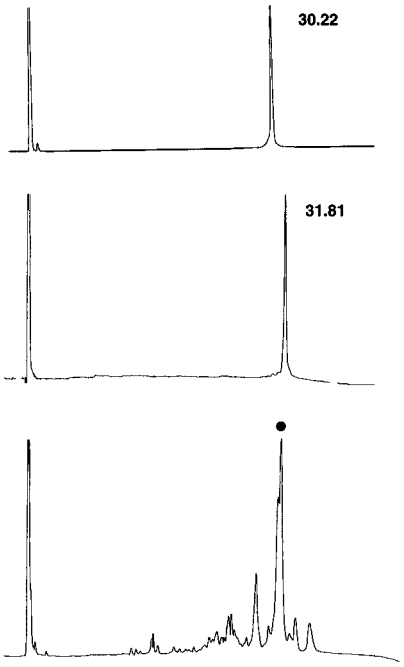

FIGURE 2: Analytical reversed-phase HPLC. (Upper panel) Apo Δ(1−43)A-I; (middle panel) apo hA-I; (lower panel) human apo HDL from which apo hA-I is purified (denoted by a closed circle above the peak). Retention times (in minutes) of the purified proteins are noted beside the peak. Elution was monitored by the absorbance at 214 nm.

by comparison to the shift observed from reduced to oxidized apo hA-I (Anantharamaiah et al., 1988; data not shown). Apo Δ(1−43)A-I has the amino acid composition and N-terminal sequence predicted from the mutagenized cDNA sequence (data not shown).

Lipid Binding and Physical Properties of Apo Δ(1−43)A-I. The lipid-associating property of apo Δ(1−43)A-I was studied by several different methods and found to be qualitatively similar to apo hA-I. The compositional analyses of purified rLphA-I and rLpΔ(1−43)A-I containing POPC ± cholesterol are shown in Table 1 and Table 2. Five to nine different preparations of each of the four possible combinations were prepared and analyzed. The compositions were very reproducible, as were the size distributions of these rLp preparations. As is normally seen for apo hA-I, these preparations are heterogeneous with respect to size and distribution (Table 1). For rLpΔ(1−43)A-I, the size distribution is shifted toward larger particles, indicating differences in lipid-bound conformation and/or protein:lipid stoichiometries per particle. There is no discernible difference in the size or distribution of the cholesterol-containing rLp compared to the respective POPC-only rLp (data not shown).

Association with human plasma lipoproteins has often been used to assess the similarity in lipid binding properties of various amphipathic peptides and apo A-I mutants to endogenous apolipoproteins (Schmidt et al., 1995; Garber et al., 1992; Ponsin et al., 1993). Radiolabeled apo hA-I or apo Δ(1−43)A-I was incubated with human plasma at either 4 °C or 37 °C and then separated by a density gradient centrifugation. As illustrated by the 4 °C incubation data (Figure 3), apo Δ(1−43)A-I has an identical distribution to apo hA-I since each appears primarily in the HDL density range. Similar experiments done at 37 °C gave identical results (data not shown). No radiolabel was apparent in any

Table 1: Analysis of Soluble and rLp Forms of Apo hA-I and Apo Δ(1−43)A-I

apolipoprotein	protein:POPC[a] ratio	Stokes diameter (nm)	distribution (%)	ΔG of binding[b] (kcal/mol)	% helix[c]	helical aa[d]
soluble hA-I				−4.9 (±1.0)	68 (±4)	165
rLphA-I	1:100(±4)	A 8.5	78			
		B 12.0	21		82 (±6)	199
		C 15.5	1			
soluble Δ(1−43)A-I				−4.6 (±0.9)	82 (±2)	165
rLpΔ(1−43)A-I	1:109(±7)	A 8.5	47			
		B 12.5	18		78 (±1)[e]	157
		C 16.5	35			

[a] Molar compositions; see Experimental Procedures for details. Values in parentheses represent standard errors. [b] The Δ*G* of binding to POPC vesicles was calculated by eq 3 under Experimental Procedures. A Student's *t*-test indicates no statistical significance ($p < 0.6$). [c] Percent helix was estimated by the method of Chen et al. (1972); the number of determinations ranged from 3 to 6. A Student's *t*-test indicates that the difference is statistically significant ($p = 0.01$). [d] The number of helical amino acids (aa) in the protein are estimated by multiplying the fractional helicity by the number of residues in the protein [apo hA-I = 243; apo Δ(1−43)A-I = 201]. [e] A Student's *t*-test indicates that there is no statistical significance between soluble and lipid-bound apo Δ(1−43)A-I ($p = 0.25$).

Table 2: LCAT Analysis of rLphA-I and rLpΔ(1−43)A-I

apolipoprotein	protein:POPC:Ch[a]	app V_{max} (nmol of CE/h)[b]	app K_m (mM protein)[b]
rLphA-I	1:98(±5):2(±0.2)	0.67 (±0.10)	0.62 (±0.01)
rLpΔ(1−43)A-I	1:95(±8):2(±0.4)	0.37 (±0.06)	0.79 (±0.18)

[a] Molar compositions; see Experimental Procedures for details. Ch = cholesterol. Values in parentheses represent standard errors. [b] The kinetic parameters are for the reaction of LCAT with the corresponding isolated cholesterol-containing rLp substrates.

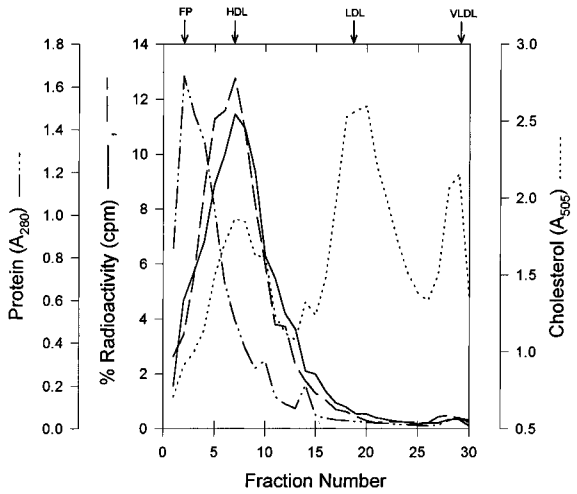

FIGURE 3: Density gradient ultracentrifugation of human plasma incubated with radiolabeled apo hA-I and Δ(1−43)A-I. Human plasma was incubated with either radioiodinated apo hA-I or apo Δ(1−43)A-I for 18 h at 4 °C followed by ultracentrifugation. The centrifuge tubes were fractionated from the bottom, and each fraction was analyzed by the absorbance at 280 nm (which principally monitors protein; − ·· −), radioactivity [to locate the position of apo hA-I,---, or apo Δ(1−43)A-I, —], and cholesterol (from a colorimetric enzymatic assay, absorbance is monitored at 505 nm, ···). The positions in the gradient where free protein (FP), HDL, LDL, and VLDL are found are indicated by arrows at the top of the figure.

other fraction nor in the free protein fraction near the tube bottom.

Surface balance measurements extend the preliminary observations made from the plasma incubation study and allow a more quantitative measure of the similarity between the lipid surface affinities of apo Δ(1−43)A-I and apo hA-I. The exclusion pressures for apo hA-I and apo Δ(1−43)A-I (the initial surface pressure at which the apolipoprotein is no longer able to penetrate the egg PC monolayer) are the

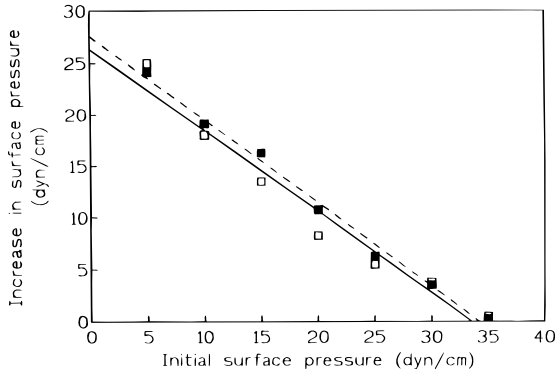

FIGURE 4: Interaction of apo hA-I and Δ(1−43)A-I with egg PC monolayers. The increases in surface pressure ($\Delta\pi$) induced by penetration of the apo A-I molecules are plotted as a function of the initial surface pressure (π_i) of the egg PC monolayer. The plotted values are the average of two measurements [■, apo hA-I; □, apo △(1−43)A-I]. The straight lines are least-squares fits to the data points [---, apo hA-I; —, apo △(1−43)A-I].

same within experimental error, 34 vs 33 dyn/cm, respectively (Figure 4). These values are close to an earlier reported value of 32 dyn/cm for apo hA-I (Ibdah & Phillips, 1988) and indicate that the proteins are equally able to penetrate an egg PC monolayer. The average equilibrium area per residue for the surface-adsorbed conformational state is obtained for increasing values of the applied surface pressure using π−A isotherms (Figure 5). At most values of π, apo Δ(1−43)A-I occupies ∼6 Å^2/residue less surface area than the monolayer of apo hA-I, indicating that the apo Δ(1−43)A-I monolayer is more condensed and that the removal of the N-terminal 43 residues affects the molecular packing of the protein within a monolayer at the air−water interface. The π−A isotherm for apo hA-I is close to that reported previously for a monolayer of apo hA-I adsorbed at the air−water interface (Krebs et al., 1988) but slightly more expanded because guanidine hydrochloride was used in the preparation of the spreading solution to prevent aggregation of the apo A-I molecules. The isotherm of apo Δ(1−43)A-I appears to have a slightly altered shape from that of apo hA-I, but whether or not this difference is significant cannot be determined because of the technical limitations of the experiment. It should be noted that compression of the protein monolayer was halted at 10 Å^2/residue because at this point the monolayer is overcompressed to a molecular area below that compatible with the existence of a protein monolayer.

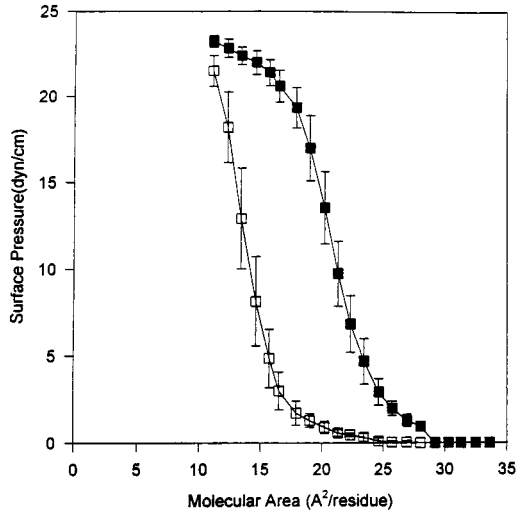

FIGURE 5: Surface pressure (π)−molecular area (A) isotherms for spread monolayers of apo hA-I and Δ(1−43)A-I at the air−water interface. Apo hA-I (■) and apo △(1−43)A-I (□). The data points are averages of at least seven determinations and are plotted ±SD.

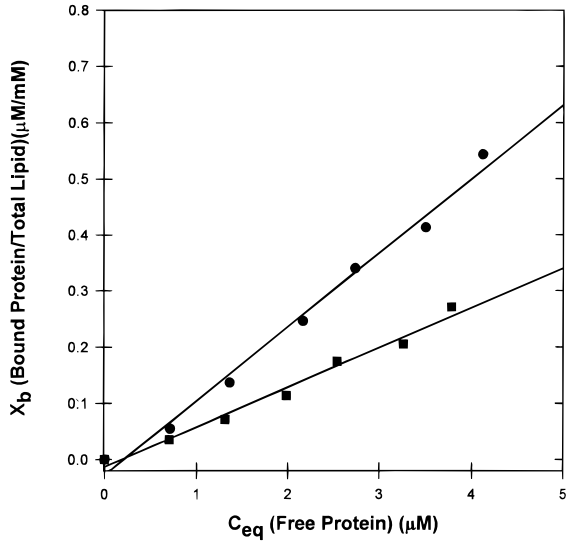

FIGURE 6: Binding of apo hA-I (●) and apo Δ(1−43)A-I (■) to POPC vesicles. The molar ratio of bound apolipoprotein to total POPC, X_b, is plotted as a function of the equilibrium concentration of unbound apolipoprotein, c_{eq}, at 4 °C. The calculated ΔG of binding for each protein is found in Table 1.

The vesicular binding assay of Spuhler et al. (1994) was performed to estimate the lipid binding affinities for the two apolipoproteins. Plots of X_b, the molar ratio of bound apolipoprotein to lipid, vs the free apolipoprotein concentration, c_{eq}, are linear ($r^2 > 0.98$) for both plots (Figure 6) (Spuhler et al., 1994). The slope of the line is equal to the binding constant, K_a (see eq 2 under Experimental Procedures), from which the binding free energy, ΔG, can be calculated (eq 3). The latter values are nearly identical for apo hA-I and apo Δ(1−43)A-I (Table 1).

Far-UV (222 nm) circular dichroism was used to compare the relative secondary structures for the lipid-free proteins versus their lipid-bound forms (Figure 7). The average percent α-helical content of apo hA-I and apo Δ(1−43)A-I, obtained from several preparations, indicates that the percent α-helical content of lipid-free apo hA-I is less than that for apo Δ(1−43)A-I (Table 1), but represents the same number of α-helical residues in each apolipoprotein. Interestingly, the extent of secondary structure in apo Δ(1−43)A-I remains

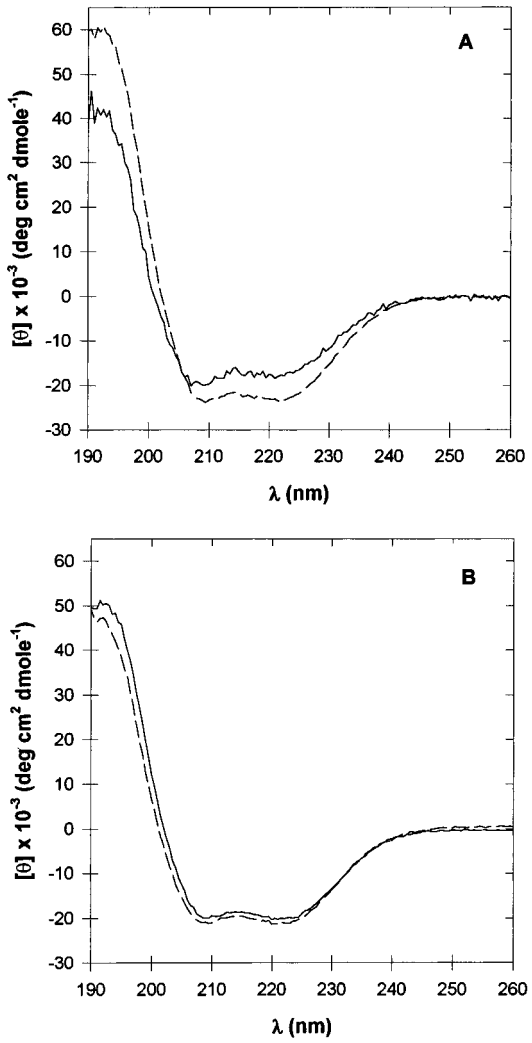

FIGURE 7: Far-UV CD of (A) apo hA-I and (B) apo Δ(1−43)A-I with (---) and without (−) POPC. The molar composition of rLp can be found in Table 1.

almost the same when bound to lipid, in contrast to apo hA-I, which acquires considerable additional α-helicity upon binding to lipid, as expected. The percent α-helix reported here for lipid-free and lipid-bound apo hA-I are typical of previously reported values from numerous laboratories (e.g., Nolte & Atkinson, 1992; Sparks et al., 1992a,b; Dalton & Swaney, 1993; Ji & Jonas, 1995; Meng et al., 1995).[2]

To assess changes in LCAT activation, which would reflect either relative changes in structure or the elimination of the LCAT activating domain caused by the deletion, isolated discoidal rLp, containing about 2 mol % cholesterol, were used as substrates (Table 2). Only the linear portions of the velocity versus protein concentration plots, in which no more than 5% conversion to cholesterol ester had occurred, were used to determine the initial velocity (data not shown). Table 2 summarizes the results of our preliminary kinetic analysis (see Experimental Procedures for details) which indicate small differences between the two proteins. These may, at least in part, be attributed to the inherent variability of the assay (Table 2), since the experimental values for both rLpΔ-(1−43)A-I and rLphA-I are within the range of those

[2] As pointed out by one reviewer, the range of values reported in the literature most likely reflects inter-laboratory differences often related to the type and calibration of the protein assay.

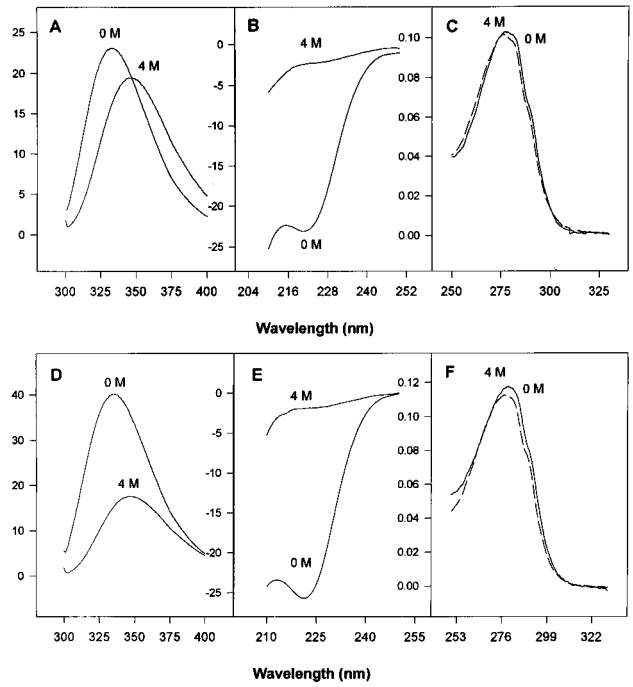

FIGURE 8: (A and D) Typical fluorescence emission spectra of apo hA-I and apo Δ(1−43)A-I, respectively, in the presence of 4.0 M urea (4 M, completely unfolded state) and in the absence of urea (0 M, native folded state). The y-axis is in fluorescence intensity units, and the *x*-axis is wavelength in nanometers. (B and E) Typical circular dichroic spectra of apo hA-I and apo Δ(1−43)A-I, respectively, in the presence of 4.0 M urea (4 M) and in the absence of urea (0 M). The *y*-axis units are molar ellipticity (degrees × $cm^2 \times dmol^{-1} \times 10^3$), and the *x*-axis is wavelength in nanometers. (C and F) Typical absorption spectra of apo hA-I and apo Δ(1−43)A-I, respectively, in the presence of 4.0 M urea (4 M, dashed line) and in the absence of urea (0 M, solid line). The *y*-axis is in absorbance units, and the *x*-axis is wavelength in nanometers.

reported for discoidal rLp containing only apo hA-I (Jonas et al., 1989; Ji & Jonas, 1995). However, the kinetic results may also reflect real differences in the intrinsic activity of the two proteins and/or differences in reactivity of the substrate resulting from the size heterogeneity and size distribution of the reconstituted complexes prepared from the two proteins.

Measurements of Reversible Equilibrium Unfolding by Spectroscopy. Denaturation of apo hA-I and apo Δ(1−43)A-I with urea was monitored using mean residue ellipticity, $[\Theta]_{222}$, difference molar absorptivity, $\Delta\epsilon_m$, and the fluorescence emission difference. Due to the nature of the N-terminal deletion, apo Δ(1−43)A-I contains only three tryptophan, five tyrosine, and five phenylalanine residues compared to four, seven, and six, respectively, in apo hA-I. Figure 8 illustrates typical fluorescence emission, circular dichroic, and absorbance spectra of apo hA-I and apo Δ(1−43)A-I in the presence and absence of urea. The unfolded protein, in all cases, has a lower fluorescence intensity than the folded protein, and the peak wavelength shows a red shift indicating an increase in the polarity of the average environment of the tryptophans due to exposure to solvent (Figure 8, panels A and D). This is consistent with the lack of defined secondary structure in the denatured protein, as determined by CD, relative to the native protein (Figure 8, panels B and E). The absorbance spectra of apo hA-I and apo Δ(1−43)A-I show that there is a slight decrease in intensity as well as a slight blue shift in the peak wavelength in the denatured proteins [both apo hA-I and apo Δ(1−43)A-I; Figure 8, panels C and F]. The parameters ΔG_{H_2O}, m_D, and $[\text{urea}]_{1/2}$ for each protein were globally fitted to the combined data sets (see Figure 9 legend) using a two-state model (Figure 9 and Table 3). Data from the urea-induced unfolding of apo hA-I versus apo Δ(1−43)A-I show that the amino-terminal truncation has a profound affect on the stability of the protein, resulting in a ΔG_{H_2O} of 4.5 ± 0.24 kcal/mol for apo Δ(1−43)A-I compared to 9.3 ± 0.88 kcal/mol for apo hA-I.

ANS Binding. The binding of the apolar dye ANS to apo hA-I and apo Δ(1−43)A-I is associated with an enhanced

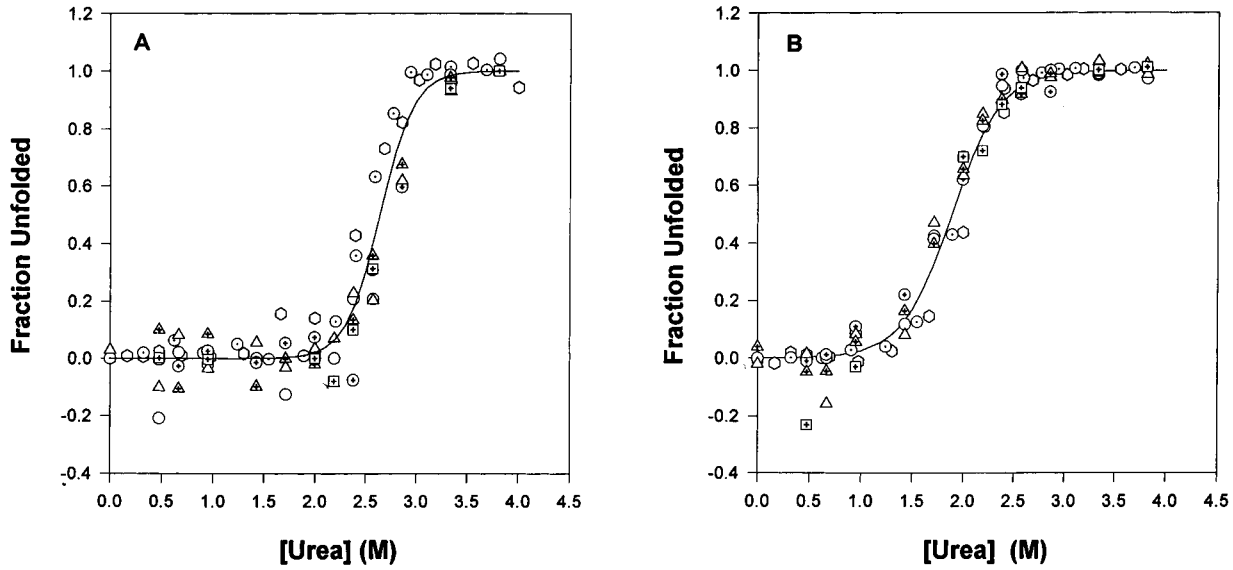

FIGURE 9: Urea-induced unfolding of apo hA-I (panel A) and apo Δ(1−43)A-I (panel B) monitored using three types of spectroscopic measurements: fluorescence emission, absorbance, and circular dichroism. In order to combine the various difference spectral measurements on a single scale for a global fitting, the experimental data were normalized to the apparent fraction of unfolded protein, f_u, as a function of urea concentration using eq 7. Symbols represent unfolding and refolding experiments monitored by absorbance (○, ⬡, and ⊙, open square with plus sign; unfolding and refolding, respectively); fluorescence (open triangle with plus sign and △; unfolding and refolding, respectively); and circular dichroism (⊕; unfolding only). The solid line represents the global two-state fits where multiple sets of data for each protein are combined to determine a single set of thermodynamic parameters (Table 3).

Table 3: Thermodynamic Parameters Associated with Apo hA-I and Apo Δ(1−43)A-I

apolipoprotein	ΔG_{H_2O}[a] (kcal/mol)	m_D[a] (kcal mol^{-1} M^{-1})	$[urea]_{1/2}$ (M)	λ_{max}[b] (nm)
apo hA-I	9.37 ± 0.56	3.55 ± 0.34	2.6	469
apo Δ(1−43)A-I	4.49 ± 0.24	2.41 ± 0.12	1.9	464
carbonic anhydrase[c]	nd	nd	nd	515

[a] A Student's *t*-test indicates there is a statistical significance ($p > 0.01$) between the numbers obtained for apo hA-I and apo Δ(1−43)A-I. [b] ANS binding. [c] Included for purposes of comparison.

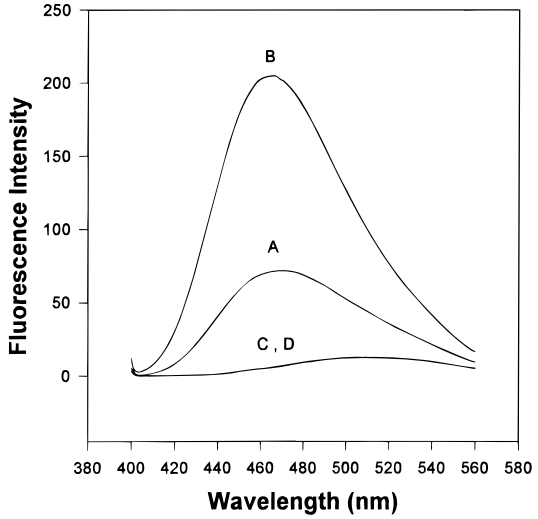

FIGURE 11: Near-UV CD of apo hA-I (□) and apo △(1−43)A-I (○), to detect differences in the asymmetric environments surrounding aromatic amino acids.

FIGURE 10: ANS binding experiments to (A) apo hA-I, (B) apo Δ(1−43)A-I, (C) carbonic anhydrase, and (D) ANS in buffer alone monitored by fluorescence emission.

fluorescence and a blue shift in the wavlength of peak emission (λ_{max}) (Figure 10 and Table 3). ANS in aqueous solution (PBS) has a quantum yield of 0.004 and an emission maximum at 515 nm (Goto & Fink, 1989). After binding to apo hA-I, there is an approximate 70-fold increase in fluorescence intensity, and a blue shift from 515 to 469 nm. There is an even more substantial increase in fluorescence intensity when ANS binds to apo Δ(1−43)A-I; approximately 200-fold increase in fluorescence intensity with a concomitant blue shift from 515 to 464 nm. This substantial increase in fluorescence intensity indicates binding to the proteins, presumably to an exposed hydrophobic surface or cavity (Stryer, 1965), and is characteristic of ANS binding to protein folding intermediates, e.g., molten globules (Semisotnov et al., 1987; Goto & Fink, 1989). In contrast, no change in fluorescence is associated with ANS binding to carbonic anhydrase (λ_{max} at 515 nm) which provides a control as a stably folded globular protein of similar size (Semisotnov et al., 1987).

Near-Ultraviolet Circular Dichroism. Near-UV circular dichroic spectra (250−330 nm), which give information on the relative asymmetrical environments of the aromatic residues in the tertiary structures of proteins, exhibit a series of positive and negative extrema which reflect the contributions of the various aromatic amino acid residues and are an indication that both proteins have a folded tertiary structure. Generally, tryptophans in proteins give rise to typical fine structured bands between 310 and 287 nm due to the ^1L_a and ^1L_b transitions (Strickland, 1974). For apo hA-I and apo Δ(1−43)A-I, these vibronic transitions are observed at 295 and 287 nm, respectively (Figure 11). The transitions at 273 and 284 nm (which appear as shoulders in both spectra) reflect contributions from both tryptophanyl and tyrosinyl residues. The characteristic fine transitions of phenylalanine are found between 250 and 265 nm. The overall spectra for apo hA-I versus apo Δ(1−43)A-I are very different, including a slight blue shift of the tryptophan signature (^1L_a and ^1L_b bands) in apo Δ(1−43)A-I. These differences in the spectral shape are probably due to environmental perturbations that shift the ^1L_a band relative to the ^1L_b band, whereas differences in intensity are more likely due to changes in side chain mobility (Strickland, 1974).

DISCUSSION

Numerous structural studies of native apo hA-I have focused on its lipid-bound structure. Some of these have addressed the importance of specific residues or helical domains outside the amino-terminal region to lipid binding and LCAT activation. Very few structural studies have focused on lipid-free apo hA-I. The present studies, therefore, are the first to provide insight into the role of the amino-terminal 43 residues, derived from exon 3, in the structure and the function of apo hA-I. It should be kept in mind that although the genomic structures of the exchangeable apolipoproteins (i.e., A-I, A-II, A-IV, C-I, C-II, C-III, and E) are highly conserved, there are distinct traits that make apo A-I unique. Analysis of the amphipathic helical classes derived from exon 3 shows that different classes are encoded by exon 3 in the different apolipoproteins (Segrest et al., 1992). For apo A-I, exon 3-derived amphipathic helices are more similar to those found in soluble, globular proteins (class G*) while the amphipathic helical class with the strongest potential for lipid binding (class A) is found exclusively in the exon 4-derived region of apo A-I. In contrast, class A helices are found exclusively in the exon 3-derived sequence of apo C-I and apo C-II. Therefore, generalizations from the present studies to the function of exon 3 residues found in other apolipoproteins would not be appropriate. The major conclusions, which will be discussed in turn, can be simply stated. (1) The lipid-bound conformations of the residues shared by apo hA-I and apo

Δ(1−43)A-I are functionally the same (i.e., residues 44−243). (2) Both lipid-free apo hA-I and apo Δ(1−43)A-I have a folded, cooperative tertiary structure, and these conformations are distinctly different.

Lipid-Bound Conformations of Apo hA-I and Apo Δ(1−43)A-I. Four independent experiments support the conclusion that both the native and mutant proteins have similar lipid binding capacities and retain similar lipid-bound conformations of their shared residues. First, apo Δ(1−43)A-I associates only with plasma HDL, as does apo hA-I, when incubated with whole human plasma (Figure 3). Second, the exclusion pressures observed when the two proteins are complexed with the egg PC monolayers are indistinguishably the same (Figure 4). Third, the estimated free energies for binding of the two proteins to POPC vesicles are nearly identical [−4.9 ± 1.0 kcal/mol and −4.6 ± 0.9 kcal/mol for apo hA-I and apo Δ(1−43)A-I, respectively; Figure 6]. Fourth, our investigation shows apo Δ(1−43)A-I form rLps in a similar range of size but, interestingly, with a different size distribution, when qualitatively compared to rLphA-I (Table 1). The differences in size heterogeneity (Table 1) of these particles might indicate differences in the preferred lipid-bound conformation of apo Δ(1−43)A-I on each species, it might also be indicative of differences due to the number of apo Δ(1−43)A-I molecules per disk. In either case, the observed similarities in lipid binding capacity do not preclude the possibility that the amino-terminal residues interact with other regions of the protein nor do they exclude the potential of this region to bind lipid.

The ability to activate LCAT has proven to be a useful benchmark in comparing different apo A-I molecules. Major differences in the lipid-bound structures would be reflected in the kinetic parameters associated with the activation of LCAT if the amino terminus plays an important role in this process. LCAT activation studies show small differences in the Michaelis−Menten kinetic parameters for cholesterol esterification using cholesterol-containing rLpΔ(1−43)A-I and rLphA-I substrates with the same POPC/cholesterol/A-I molar compositions; rLpΔ(1−43)A-I is 2-fold less reactive than rLphA-I (Table 2). It is important to view these results as preliminary observations since the substrates used were heterogeneous with respect to size. It has been shown that the size of rLphA-I influences LCAT activity because of differences in the conformation of the associated apo A-I molecules (Jonas et al., 1990; Meng et al., 1993; Sparks et al., 1995). Therefore, it is possible that differences in the size distribution and/or stoichiometric heterogeneity observed for rLphA-I and rLpΔ(1−43)A-I are responsible for the slight decrease in reactivity of rLpΔ(1−43)A-I. It will be necessary to study homogeneous complexes to distinguish possible differences in intrinsic activity of the two proteins from differences resulting from size and/or stoichiometric heterogeneity. For example, it is conceivable that larger differences in activity will be apparent once complexes of the same size and stoichiometry are compared. However, the finding that rLpΔ(1−43)A-I retains the ability to activate LCAT makes it unlikely that residues 1−43 are intrinsically necessary for directly activating LCAT, nor are they likely to play a critical role in maintaining the correct structure of the domain(s) involved in activating LCAT. Subtle differences in the lipid-bound conformations of these proteins will be explored in future studies. When taken together with data from other labs (Ji & Jonas, 1995), our results suggest that the domains important for LCAT activation reside between residues 43 and 187.

Lipid-Free Conformations of Apo hA-I and Apo Δ(1−43)A-I. Substantial differences in conformation were observed for the two proteins in their lipid-free states. The absence of the amino-terminal 43 residues increases the helicity and the ability for this protein to be more compact, probably through a rearrangement of the overall tertiary structure. Further, apo Δ(1−43)A-I has a much less stable tertiary conformation than apo hA-I, as judged by urea-induced unfolding, which also indicates a significant change in the conformation of the mutant protein. These observations suggest part or all of the amino-terminal 43 residues are an integral structural element in the conformation of lipid-free apo hA-I. ANS binding experiments indicated that the hydrophobic residues in apo Δ(1−43)A-I are much more accessible to solvent, consistent with a loose structure that is only weakly stabilized by tertiary interactions, an interpretation which is consistent with the lower stability.

It is concluded from CD measurements on the lipid-free and lipid-bound states of the two proteins that different residues are helical in their respective lipid-free conformations. The percent helicity of lipid-free apo Δ(1−43)A-I is 82% compared to 68% for apo hA-I (Table 1); however, the proteins contain the same number of residues in a helical conformation. This could be interpreted as simply being the loss of a nonhelical region with no accompanying conformational change or, alternatively, residues that are normally nonhelical acquire helicity in the mutant protein. The first interpretation can be ruled out based on the significant decrease in stability of the mutant protein and the increased ability to bind ANS, both of which indicate a structural rearrangement. Therefore, it is possible that a large fraction of the nonhelical residues of soluble apo hA-I are probably in the extreme carboxy terminus (approximately residues 187−243, although the existence of other nonhelical regions cannot be ruled out here), because this region is preferentially proteolyzed in the lipid-free state (Leroy & Jonas, 1994; Brouillette & Anantharamaiah, 1995). It is likely that these residues acquire helicity upon binding to lipid, and this supposition is supported by experiments on C-terminally truncated apo A-I proteins, which are defective in their ability to bind to lipid (Ji & Jonas, 1995). Logically, since no significant change in helicity accompanies apo Δ(1−43)A-I binding to lipid, these carboxy-terminal residues must already be helical in the lipid-free conformational state of apo Δ(1−43)A-I. Therefore, it is more probable that residues which are nonhelical in the native protein acquire helicity in the structure of apo Δ(1−43)A-I. Thus, the absence of residues 1−43 appears to convert residues 44−243 from their lipid-free to the lipid-bound secondary structure.

Surface balance measurements suggest a more compact conformational state for apo Δ(1−43)A-I compared to apo hA-I. The organization of the apolipoprotein molecules at the air−water interface is a function of π (Ibdah & Phillips, 1988; Ibdah et al., 1989; Phillips & Krebs, 1986). At high values of π, the difference in molecular area occupied by apo hA-I and apo Δ(1−43)A-I (Figure 5) indicates that their interfacial conformations differ. The more condensed packing for the apo Δ(1−43)A-I monolayer is consistent with the molecules being more α-helical and with the helices being more closely packed due to a rearrangement of the structure. This effect could arise because in apo hA-I, the

N-terminal 43 residues interfere with the alignment of the C-terminal α-helices in the plane of the interface, thereby giving rise to the more expanded isotherm for apo hA-I. The collapse of the apo hA-I monolayer that commences at ∼18 Å^2, per residue (Figure 5) may be due to a squeezing-out from the plane of the interface of the N-terminal 43 residues. Due to the lack of this domain, apo Δ(1−43)A-I forms a monolayer of closely packed helices that does not start to collapse until the molecular area is reduced to ∼13 Å^2 per residue.

Tertiary Structures of Lipid-Free Apo hA-I and Apo Δ(1−43)A-I. The urea-induced unfolding is reversible, and fits well to a two-state process for both proteins (Figure 9), indicating folded and cooperative, tertiary structures (Privalov, 1979). However, apo Δ(1−43)A-I is much less stable than apo hA-I, with 50% of the apo Δ(1−43)A-I protein unfolded in 1.9 M urea compared to apo hA-I which has a midpoint of unfolding at 2.6 M urea (Table 3). Unlike other reported ΔG_{H_2O} values for apo hA-I, ranging from 2.2 kcal/mol to 6.8 kcal/mol (Tall et al., 1976; Edelstein & Scanu, 1980; Reijngould & Phillips, 1982; Leroy & Jonas, 1994), the values presented in this paper represent a global, nonlinear regression fit of ΔG_{H_2O} values to experimental data sets from three different types of spectroscopic measurements. Differences in the fitting procedure may explain the higher stability obtained for apo hA-I in the present studies, since refitting published data using our nonlinear regression increases the average ΔG_{H_2O} values obtained by Tall et al. (1976), for example, from a ΔG_{H_2O} value of 2.2 kcal/mol to 4.7 ± 0.22 kcal/mol. The dramatic decrease in stability of apo Δ(1−43)A-I suggests a different folding pattern than its native counterpart. Further evidence for this conclusion comes from near- and far-UV CD spectra and the relative capacities of each protein to bind to the hydrophobic probe, ANS.

The near-UV CD spectra of lipid-free apo hA-I and apo Δ(1−43)A-I are dramatically different (Figure 11) but demonstrate that both apo hA-I and apo Δ(1−43)A-I have a folded tertiary structure. Near-UV CD gives an indication of the overall asymmetry surrounding the aromatic residues, and the characteristic fine transitions in discrete regions of the spectrum represents, respectively, an average of the environments around all the tryptophans, tyrosines, and phenylalanines (Strickland, 1974). Apo hA-I contains four tryptophans, seven tyrosines, and five phenylalanines. In deleting the first 43 residues, tryptophan 8, tyrosines 18 and 29, and phenylalanine 33 have been eliminated. The pronounced change in the near-UV CD spectrum that occurs with this deletion indicates, at the least, that the aromatic residues within the 1−43 sequence contribute to the CD spectrum and, therefore, are held in an asymmetric environment produced by the folded, tertiary structure of apo hA-I. The altered near-UV CD spectrum of apo Δ(1−43)A-I may further reflect a different tertiary structure for residues 44−243 compared to their structure in apo hA-I. This latter possibility is consistent with the greater percent helicity suggested for this region by the far-UV CD. The combined near- and far-UV CD data support the conclusion that the folded core of native apo hA-I is defined by residues 1 through (approximately) 186.

Figure 10 illustrates the ability of the two proteins to bind ANS, indicating the exposure of a hydrophobic surface or pocket (Stryer, 1965). ANS does not bind to unfolded proteins (Goto & Fink, 1989) or to the native state of typical globular proteins (Stryer, 1965; Semisotnov et al., 1987). Hence, ANS binding has come to be identified with the presence of a molten globule structure (Goto & Fink, 1989), a characteristic that has also been recently suggested to apply to lipid-free apo hA-I (Gursky & Atkinson, 1996). However, the fluorescence intensity seen in apo Δ(1−43)A-I due to ANS binding is 3-fold higher than even apo hA-I, suggesting a poorly defined, nonstable tertiary structure. This property is clearly manifested in the lower thermodynamic stability.

Conclusions. The structural data on lipid-free apo Δ(1−43)A-I can be used to expand current models of the molecular mechanism for apo hA-I lipid binding. The conformational plasticity of the extreme carboxy terminus has been previously suggested (Ji & Jonas, 1995; Gursky & Atkinson, 1996) to initiate lipid binding of soluble apo hA-I, possibly mediated through a molten globule state. To reach the final lipid-bound state, this partially lipid-bound intermediate must undergo further conformational changes that expose new lipid binding domains. We propose that the amino-terminal domain of apo hA-I masks a latent lipid binding domain (i.e., a hydrophobic surface). Movement of the amino-terminal domain is a good candidate for the conformational switch that precedes the binding of the remaining helical domains to lipid, since the deletion of residues 1−43 results in a new conformation for the remainder of the protein. For lipid-free apo Δ(1−43)A-I, a helical carboxy-terminal domain (within residues 187−243) is probably required to protect or interact with the hydrophobic surface of the latent lipid binding domain (within residues 44−186) exposed by the deletion of the N-terminal 43 residues.

ACKNOWLEDGMENT

We thank Dr. Donald Muccio (UAB) for his assistance in obtaining and interpreting the CD data, Dr. John Baker, director of the Glycoprotein Analysis Core Facility at the University of Alabama at Birmingham Medical Center, for amino acid analyses and protein sequencing, Mr. Larry Ross (SRI), Ms. Sheila Benowitz (MCP) and Ms. Sridevi Alluri (UAB) for technical assistance, and Dr. Kenneth Taylor (UAB) for assistance in the kinetic analysis of the LCAT data.

REFERENCES

Acton, S., Rigotti, A., Landschulz, K. T., Xu, S., Hobbs, H. H., & Krieger, M. (1996) *Science 271*, 518−520.

Albers, J. J., Chen, C.-H., & Lacko, A. G. (1986) *Methods Enzymol. 129*, 763−783.

Anantharamaiah, G. M., Hughes, T. A., Iqbal, M., Gawish, A., Neame, P. J., Medley, M. F., & Segrest, J. P. (1988) *J. Lipid Res. 29*, 309−318.

Barbeau, D. L., Jonas, A., Teng, T., & Scanu, A. M. (1979) *Biochemistry 18*, 362−369.

Bergeron, J., Frank, P. G., Scales, D., Meng, Q.-H., Castro, G., & Marcel, Y. L. (1995) *J. Biol. Chem. 270*, 27429−27438.

Breslow, J. L. (1989) in *The Metabolic Basis of Inherited Disease* Scriver, C. R., Beaudet, A. L., Sey, W. S., Valle, D., Eds.) 7th ed., pp 1251−1266, McGraw-Hill, Inc., New York.

Brouillette, C. G., & Anantharamaiah, G. M. (1995) *Biochim. Biophys. Acta 1256*, 103−129.

Brouillette, C. G., Jones, J. L., Kercret, H., Ng, T. C., & Segrest, J. P. (1984) *Biochemistry 23*, 359−367.

Bruhn, H., & Stoffel, W. (1991) *Biol. Chem. Hoppe-Seyler 372*, 225−234.

Calabresi, L., Meng, Q.-H., Castro, G. R., & Marcel, Y. L. (1993) *Biochemistry 32*, 6477−6484.

Chen, Y.-H., Yang, J. T., & Martinez, H. M. (1972) *Biochemistry 11*, 4120−4131.
Cheung, P., & Chan, L. (1983) *Nucleic Acids Res. 11*, 3703−3715.
Collet, H., Perret, B., Simard, G., Raffai, E., & Marcel, Y. L. (1991) *J. Biol. Chem. 266*, 9145−9152.
Curtiss, L. K., & Smith, R. S. (1988) *J. Biol. Chem. 263*, 13779−13785.
Dalton, M. B., & Swaney, J. B. (1993) *J. Biol. Chem. 268*, 19274−19283.
Edelstein, C., & Scanu, A. M. (1980) *J. Biol. Chem. 255*, 5747−5754.
Eftink, M. R. (1994) *Biophys. J. 66*, 482−501.
Fielding, C. J., Shore, V. G., & Fielding, P. E. (1972) *Biochem. Biophys. Res. Commun. 46*, 1493−1498.
Forte, T. M., & McCall, M. R. (1994) *Curr. Opin. Lipidol. 5*, 354−364.
Garber, D. W., Venkatachalapathi, Y. V., Gupta, K. B., Ibdah, J., Phillips, M. C., Hazelrig, J. B., Segrest, J. P., & Anantharamaiah, G. M. (1992) *Arterioscler. Thromb. 12*, 886−894.
Glomset, J. A. (1968) *J. Lipid Res. 9*, 155−167.
Gordon, T., Castelli, W. P., Hjortland, M. C., Kannel, W. B., & Dawber, T. R. (1977) *Am. J. Med. 62*, 707−714.
Goto, Y., & Fink, A. L. (1989) *Biochemistry 28*, 945−952.
Gursky, O., & Atkinson, A. (1996) *Proc. Natl. Acad. Sci. U.S.A. 93*, 2991−2995.
Hughes, T. A., Moore, M. A., Neame, P., Medley, M. F., & Chung, B. H. (1988) *J. Lipid Res. 29*, 363−376.
Ibdah, J. A., & Phillips, M. C. (1988) *Biochemistry 27*, 7155−7162.
Ibdah, J. A., Krebs, K. E., & Phillips, M. C. (1989) *Biochim. Biophys. Acta 1004*, 300−308.
Ji, Y., & Jonas, A. (1995) *J. Biol. Chem. 270*, 11290−11297.
Jonas, A., Kezdy, K. E., & Wald, J. H. (1989) *J. Biol. Chem. 264*, 4818−4824.
Jonas, A., Wald, J. H., Toohill, K. L. H., Krul, E. S., & Kezdy, K. (1990) *J. Biol. Chem. 265*, 22123−22129.
Krebs, K. E., Ibdah, J. A., & Phillips, M. C. (1988) *Biochim. Biophys. Acta 959*, 229−237.
Leroy, A., & Jonas, A. (1994) *Biochim. Biophys. Acta 1212*, 285−294.
Li, W.-H., Tanimura, M., Luo, C.-C., Datta, S., & Chan, L. (1988) *J. Lipid Res. 29*, 245−271.
Marcel, Y. L., Provost, P. R., Koa, H., Raffai, E., Vu Dac, N., Fruchart, J.-C., & Rassart, E. (1991) *J. Biol. Chem. 266*, 3644−3653.
Matz, E. E., & Jonas, A. (1982) *J. Biol. Chem. 257*, 4535−4540.
McFarland, A. S. (1958) *Nature 182*, 53.
McLachlan, A. D. (1977) *Nature 267*, 465−466.
Meng, Q.-H., Calabresi, L., Fruchart, J.-C., & Marcel, Y. L. (1993) *J. Biol. Chem. 268*, 16966−16973.
Meng, Q.-H., Bergeron, J., Sparks, D. L., & Marcel, Y. L. (1995) *J. Biol. Chem. 270*, 8588−8596.
Minnich, A., Collet, X., Roghani, A., Cladaras, C., Hamilton, R. L., Fielding, C. J., & Zannis, V. I. (1992) *J. Biol. Chem. 267*, 16553−16560.
Nolte, R. T., & Atkinson, D. A. (1992) *Biophys. J. 63*, 1221−1239.
Oram, J. F. (1986) *Methods Enzymol. 129*, 645−659.
Osborne, J. C., & Brewer, H. B., Jr. (1977) *Adv. Protein Chem. 31*, 253−337.
Pace, C. N., Shirley, B. A., & Thomson, J. A. (1989) in *Protein Structure: a practical approach* (Creighton, T. E., Ed.) pp 311−330, Oxford University Press, Oxford, England.
Phillips, M. C., & Krebs, K. E. (1986) *Methods Enzymol. 128*, 387−403.
Plumb, A. S., Scott, C. J., & Breslow, J. L. (1994) *Proc. Natl. Acad. Sci. U.S.A. 91*, 9607−9611.
Ponsin, G., Pulcini, T., Sparrow, J. T., Gotto, A. M., Jr., & Pownall, H. J. (1993) *J. Biol. Chem. 268*, 3114−3119.
Pownall, H. J., & Massey, J. B. (1986) *Methods Enzymol. 128*, 515−518.
Radin, N. S. (1981) *Methods Enzymol. 72*, 5−7.
Reijngoud, D.-J., & Phillips, M. C. (1982) *Biochemistry 21*, 2969−2976.
Santoro, M. M., & Bolen, D. W. (1988) *Biochemistry 27*, 8063−8068.
Schmidt, H. H.-J., Remaley, A. T., Stonik, J. A., Ronan, R., Wellmann, A., Thomas, F., Zech, L. A., Brewer, H. B., Jr., & Hoeg, J. M. (1995) *J. Biol. Chem. 270*, 5469−5475.
Schultz, J. R., Verstuyft, J. G., Gong, E. L., Nichols, A. V., & Rubin, E. M. (1993) *Nature 365*, 762−764.
Segrest, J. P., Jones, M. K., De Loof, H., Brouillette, C. G., Venkatachalapathi, Y. V., & Anantharamaiah, G. M. (1992) *J. Lipid Res. 33*, 141−166.
Segrest, J. P., Garber, D. W., Brouillette, C. G., Harvey, S. C., & Anantharamaiah, G. M. (1994) *Adv. Protein Chem. 45*, 303−369.
Semisotnov, G. V., Rodionova, N. A., Razgulyaev, O. I., Uversky, V. N., Gripas, A. F., & Gilmanshin, R. I. (1991) *Biopolymers 31*, 119−128.
Sorci-Thomas, M., Kearns, M. W., & Lee, J. P. (1993) *J. Biol. Chem. 268*, 21403−21409.
Sparks, D. L., Phillips, M. C., & Lund-Katz, S. (1992a) *J. Biol. Chem. 267*, 25830−25838.
Sparks, D. L., Lund-Katz, S., & Phillips, M. C. (1992b) *J. Biol. Chem. 267*, 25839−25847.
Sparks, D. L., Anantharamaiah, G. M., Segrest, J. P., & Phillips, M. C. (1995) *J. Biol. Chem. 270*, 5151−5157.
Spuhler, P., Anantharamaiah, G. M., Segrest, J. P., & Seelig, J. (1994) *J. Biol. Chem. 269*, 23904−23910.
Strickland, E. H. (1974) *CRC Crit. Rev. Biochem. 2*, 113−175.
Stryer, L. (1965) *J. Mol. Biol. 13*, 482−495.
Studier, F. W., & Moffat, B. A. (1986) *J. Mol. Biol. 189*, 113.
Sviridov, D., Pyle, L., & Fidge, N. (1996) *Biochemistry 35*, 189−196.
Tall, A. R., Shipley, G. G., & Small, D. M. (1976) *J. Biol. Chem. 251*, 3749−3755.
Tendian, S. W., Myszka, D. G., Sweet, R. W., Chaiken, I. W., & Brouillette, C. G. (1995) *Biochemistry 34*, 6464−6474.
Vieira, J., & Messing, J. (1987) *Methods Enzymol. 153*, 3.
Warden, C., Hedrick, C. C., Quao, J.-H., Castellani, L. W., & Lusis, A. J. (1993) *Science 261*, 469−471.
Warnick, G . R. (1986) *Methods Enzymol. 129*, 101−123.
Warren, J. R., & Gordon, J. A. (1966) *J. Phys. Chem. 70*, 297−300.
Zoller, M. J., & Smith, M. (1983) *Methods Enzymol. 100*, 468.

BI961876E